Catalysis Today 136 (2008) 222–227

Contents lists available at ScienceDirect

Catalysis Today

journal homepage: www.elsevier.com/locate/cattod

Development of *iso*-octane fuel processor system for fuel cell applications

Dong Ju Moon *, Jong Woo Ryu, Kye Sang Yoo, Dae Jin Sung, Sang Deuk Lee

Clean Energy Research Center, Korea Institute of Science and Technology (KIST), P.O. Box 131, Cheongrayang, Seoul 130-650, Republic of Korea

ARTICLE INFO

Article history:
Available online 1 May 2008

Keywords:
iso-Octane fuel processor
Autothermal reforming (ATR)
High temperature shift (HTS)
Low temperature shift (LTS)
iso-Octane

ABSTRACT

An *iso*-octane fuel processor system with three different reaction stages, autothermal reforming (ATR) reaction of *iso*-octane, high temperature shift (HTS) and low temperature shift (LTS) reactions, was developed for applications in a fuel cell system. Catalytic properties of the prepared Ni/Fe/MgO/Al_2O_3 and Pt–Ni/CeO_2 or molybdenum carbide catalysts were compared to those of commercial NiO/CaO/Al_2O_3 and Cu/Zn/Al_2O_3 catalysts for ATR and LTS reaction, respectively. It was found that the prepared catalysts formulations in the fuel processor system were more active than those of the commercial catalysts. As the exit gas of *iso*-octane ATR over the Ni/Fe/MgO/Al_2O_3 catalyst was passed through Fe_3O_4–Cr_2O_3 catalyst for HTS and Mo_2C or Pt–Ni/CeO_2 catalyst for LTS reaction, the concentration of CO in hydrogen-rich stream was reduced to less than 2400 ppm. The results suggest that the *iso*-octane fuel processor system with prepared catalysts can be applied to PEMFC system when a preferential partial oxidation reaction is added to KIST *iso*-octane reformer system.

1. Introduction

Hydrogen is the ideal fuel for the stationary and auxiliary fuel cell-powered units as well as a proton exchanged membrane (PEM) fuel cell. Recently, PEM fuel cells operating with H_2 from steam reforming or partial oxidation of hydrocarbon are being increasingly accepted as the most appropriate power source for future generation vehicles. The successful development of a fuel cell-powered vehicle or of stationary fuel cell-powered units is dependent on the development of a fuel processor [1,2].

A direct hydrogen system has many disadvantages such as the lack of widespread refueling infrastructure and high storage volume compared to the hydrocarbon based fuels such as methanol and gasoline. It is known that methanol yields the highest vehicle efficiencies among all the available liquid fuels [1–3]. However, gasoline is the best candidate fuel for the fuel cell-powered vehicle, because the lower efficiency of gasoline in comparison with methanol can be compensated by its much higher energy density compared to methanol and also by its well developed infrastructure [2,3].

Major process technologies for reforming hydrocarbons and alcohols into hydrogen, carbon monoxide and carbon dioxide are catalytic steam reforming (SR), partial oxidation (POX) and autothermal reforming (ATR) [2–4]. Steam-reforming reaction of hydrocarbon usually takes place at temperature around 700 °C at which it shows the highest reforming efficiency. But the drawback is that this reaction is an endothermic and therefore, the reactor needs to be heated by combustion of fuels itself. Recently, the results of an investigation carried out to develop sulfur-tolerant reforming catalyst were reported [5–7]. However, no sulfur tolerant steam-reforming catalyst has been designed especially in the presence of high sulfur-containing fuel feeds, resulting in need of a very efficient and therefore probably large unit for removing the sulfur contained in fuels [2,5–7]. POX and ATR systems do not require external heating and can be heated up internally relatively quickly by exothermic reaction of fuels. Hence they are more dynamic than steam-reforming system. The sulfur tolerance for ATR system is also better than that of steam reforming. Also, the ATR process attracts much attention primarily due to the low energy requirement, the opposite contribution of the exothermic hydrocarbon oxidation, endothermic steam-reforming reaction and also due to the high space velocity compared to the POX process [8].

The water gas shift (WGS) reaction is one of the key catalytic stages in a fuel processor. Its function is to reduce the carbon monoxide concentration, at the same time increasing hydrogen content. Since the reaction is an exothermic, the equilibrium CO conversion is highest at low temperature. Consequently, a two-stage process is often used [9–11]. In industrial reactors, Fe_3O_4–Cr_2O_3 and Cu–Zn/Al_2O_3 catalysts are used for the high temperature shift (HTS) and for the low temperature shift (LTS) reactions, respectively. The reaction is moderately exothermic with $\Delta H = -41.1$ kJ/mol [10]. The water gas shift reaction is usually carried out in two adiabatic shift reactors, the high temperature

* Corresponding author. Tel.: +82 2 958 5867.
E-mail address: djmoon@kist.re.kr (D.J. Moon).

0920-5861/$ – see front matter © 2008 Elsevier B.V. All rights reserved.
doi:10.1016/j.cattod.2008.02.022

shift reactor and the low temperature shift reactor, separated by an intercooler in between. In our previous work, we have reported [12–15] the development of a gasoline fuel processor including ATR over a commercial ICI reforming catalyst, high temperature water gas shift reaction over Fe_3O_4–Cr_2O_3 catalyst and low temperature shift reaction over $Cu/ZnO/Al_2O_3$ catalyst. We have pointed out the necessity of development of high performance, coke and sulfur-resistant ATR and LTS catalysts, the various experimental features of the gasoline processor as well as the goals to be achieved in the near future.

In present study, we have selected *iso*-octane, a principal constituent in gasoline as a fuel feed. So the results obtained over *iso*-octane feed can be used to develop an *iso*-octane fuel processor system. We have carried out the ATR reaction of *iso*-octane, high temperature water gas shift reaction and low temperature shift reaction, and developed the *iso*-octane fuel processor system with three different reaction stages for integration with PEM fuel cell and SOFC based systems. *iso*-Octane fuel processor system charged with prepared catalyst was compared with those charged with commercial ATR and LTS catalysts, respectively.

2. Experimental

2.1. Chemical

The *iso*-octane as a fuel source was supplied by J.T. Baker. The standard *iso*-octane feed containing 100 ppm of sulfur was prepared by mixing of requisite amount of thiophene (99%+, Acros Organics) to *iso*-octane. Hydrogen (99.999%), air (99.999%) and nitrogen (99.999%) were used in the reaction and for the pretreatment of catalysts. Nickel nitrate, ferric nitrate, ammonium molybdate and magnesium hydrate were procured from Sigma–Aldrich Co. Also, γ-alumina (2–3 μm) was obtained from High Purity Chemicals.

2.2. Catalysts

The commercial ATR catalyst ($NiO/CaO/Al_2O_3$) for *iso*-octane reforming, HTS (Fe_3O_4–Cr_2O_3) and LTS ($Cu/ZnO/Al_2O_3$) catalysts for clean up of CO were obtained from ICI in the form of pellets. However, all catalysts in this work were pressed, crushed and particles with a mesh size of 120/230 were selected for the reaction.

The KIST ATR ($Ni/Fe/MgO/Al_2O_3$) catalyst was prepared by the method of incipient wetness of the γ-alumina with aqueous solutions of the corresponding metal nitrates [12,13]. Molybdenum carbide catalyst was synthesized by the temperature-programmed carburization method of molybdenum oxide [16–18]. Pt–Ni/CeO_2 catalyst was prepared by incipient wetness method.

2.3. Catalyst characterization

BET surface area and total pore volume of catalysts before and after the reaction of *iso*-octane were measured by N_2 physisorption. Active metal surface area of catalyst was calculated by CO chemisorption using a sorption analyzer (Quantachrome Co., Autosorb-1C). Structure of the catalysts before and after the reaction was analyzed by a XRD analyzer (Shimazdu Co., XRD-6000).

2.4. iso-Octane fuel processor system

The schematic diagram of an *iso*-octane fuel processor system is shown in Fig. 1. Also, Fig. 2 shows a photograph of *iso*-octane fuel processor system designed by KIST. It consists of six sections: feed supply, evaporator, ATR reactor, HTS reactor, LTS reactor and GC analysis sections. The gases were delivered by mass flow controllers, whereas, H_2O and liquid fuels were fed by liquid delivery pumps (Young Lin Co., model M930). Both evaporator and ATR reactor were made up of an Inconel 600 tube (0.0095-m i.d. and 0.20-m length), HTS and LTS reactors made up of Inconel 600 tube (0.0075-m i.d. and 0.20-m length) were employed in this study. The temperature of evaporator, ATR, HTS and LTS reactors was controlled by a PID temperature controller and was monitored by a separate thermocouple placed in the catalyst bed. This arrangement was capable of ensuring the accuracy of ±1 °C of the catalyst bed temperature. Unreacted H_2O was removed by an ice trap and then gas effluent was analyzed by on-line GC.

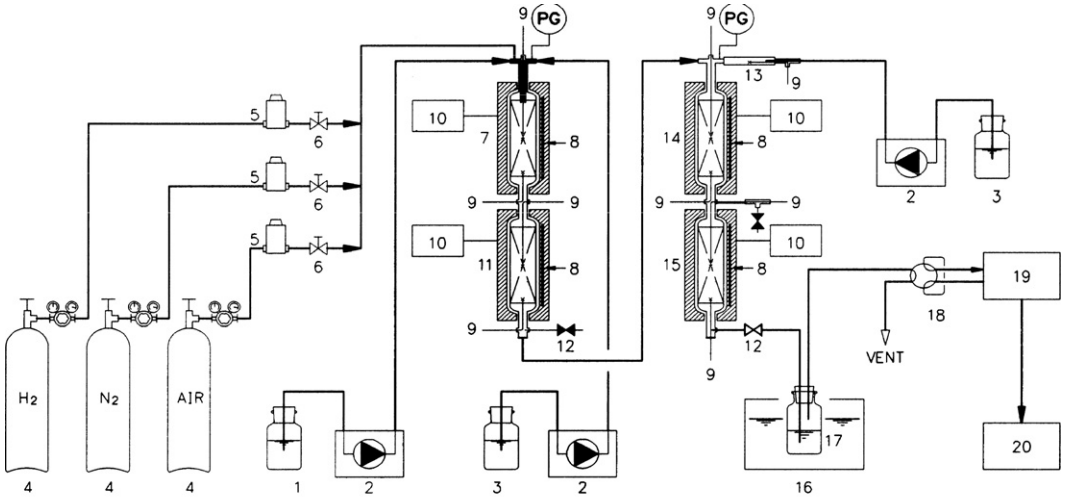

Fig. 1. A schematic diagram of *iso*-octane fuel processor system.

Fig. 2. A photograph of *iso*-octane fuel processor system.

2.5. Activity measurements

For a typical reaction, 1 g of ATR catalyst was charged in the Inconel reactor and pretreated for 1 h at 700 °C under a hydrogen flow rate of 60 cm^3/min. All iso-octane fuel processor runs were conducted in the temperature range of 550–750 °C, space velocity of 8776 h^{-1}, feed molar ratios of $H_2O/C = 3$ and $O/C = 1$, and at atmospheric pressure. The vaporized fuel and water were mixed with air and passed over the heated catalyst zone. We also carried out the stability test of the reforming catalyst to check carbon deposition and sulfur tolerance levels. To reduce CO concentration, the exit gas from the ATR reactor was passed into HTS reactor for WGS reaction. The exit stream from HTS reactor was then cooled and passed into LTS reactor. The LTS catalyst was reduced at 200 °C in a mixture of 2% H_2 in N_2 balance for 4.5 h. The gas effluent was analyzed by on-line gas chromatograph (HP-6890 Series II) equipped with TCD and Carbosphere column (0.0032-m o.d. and 3.048-m length, 80/100 meshes). The species concentration in the exit of ATR reactor, HTS and LTS was calculated on a dry basis by the gas chromatography. Water could not be analyzed during the reaction, because its analysis by chromatography was not reliable, which it is at the same time a reactant and a reaction product.

3. Results and discussion

3.1. ATR reaction

The catalyst formulations used in this work and their characteristics are summarized in Table 1. BET surface area and active metal surface area of $Ni/Fe/MgO/Al_2O_3$ catalyst were found to be higher (74 and 1.906 m^2/g) than those of the commercial ICI catalyst (35 and 0.186 m^2/g), respectively. BET surface area and active metal surface area of Mo_2C catalyst was similar to that of $Cu–Zn/Al_2O_3$ catalyst.

In our previous work [12–15], we carried out ATR reaction of *iso*-octane, HTS and LTS reactions over commercial catalysts, and investigated the effect of the operating conditions such as reaction temperature, O/C molar ratio, H_2O/C molar ratio, space velocity and the effect of impurities contained in fuels. It was reported that reaction temperature of 700 °C, feed molar ratios of $H_2O/C = 3$ and $O/C = 1$ were favorable for the ATR reaction of *iso*-octane over the commercial catalyst.

In our previous work [12–15], the problems of catalyst deactivation by carbon deposition and sulfur poisoning in the ATR reaction of *iso*-octane over the commercial reforming catalyst was reported. We investigated various supported transition metal formulations which are coke- and sulfur-resistant for ATR reaction of *iso*-octane [15]. Especially, the catalyst formulations with $Ni/Fe/MgO/Al_2O_3$ displayed reasonably good activity towards the ATR reaction of *iso*-octane. The hydrogen selectivity of some systems was much higher than that of the commercial ICI and HT catalysts under the tested conditions [12,13].

We compared the KIST catalyst ($Ni/Fe/MgO/Al_2O_3$) with the commercial ICI catalysts for the product distribution in the ATR reaction of *iso*-octane [12]. The ATR reaction over KIST and commercial ICI catalysts were carried out at 700 °C with a space velocity of 8776 h^{-1} and feed molar ratios of $H_2O/C = 3$ and $O/C = 1$. The product distribution over KIST catalyst is similar to that over commercial ICI catalyst. In case of systems possessing Ni as the major component, both Fe and Co are very effective components, which in very small amounts can considerably enhance the performance of the Ni-based systems [12,13]. The considerable enhancement of the H_2 selectivity over the nickel based systems doped with small amounts of other active components may be caused by a synergistic effect of the active components and supports, resulting in the proper dispersion of the active components thereby, providing more active sites for the reaction [14].

In our previous work [12], it was found that Ni-based systems doped with small amounts Fe and/or Co displayed reasonably high H_2 selectivity for ATR reaction of *iso*-octane containing 5 ppm sulfur. These catalysts showed higher H_2 selectivity and lower CO selectivity than a commercial ICI catalyst tested under the same conditions. Fig. 3 shows the long-term stability of KIST ($Ni/Fe/MgO/Al_2O_3$) and commercial ICI catalysts for the ATR of *iso*-octane containing sulfur less than 5 ppm at 700 °C with molar ratios of $H_2O/C = 3$ and $O/C = 1$ over 760 h [12]. Conversion of *iso*-octane was more than 99.9% for 760 h. We could not find any change in the product distributions over the KIST and commercial ICI catalysts during the time period investigated. It was observed that the KIST catalyst ($Ni/Fe/MgO/Al_2O_3$) has been stable for the ATR of *iso*-octane containing sulfur less than 5 ppm under the experimented reaction conditions.

Table 1
Characteristics of the prepared and the commercial catalysts

Catalysts	Reaction	BET surface area (m^2/g)[a]	Total pore volume (cm^3/g)[a]	Active metal surface area (m^2/g)[b]	Maker
$NiO/CaO/Al_2O_3$	ATR	35	0.085	0.186	ICI
$Ni/Fe/MgO/Al_2O_3$	ATR	74	0.212	1.906	KIST
$Fe_3O_4–Cr_2O_3$	HTS	57	0.073	0.127	ICI
$Cu–Zn/Al_2O_3$	LTS	60	0.081	0.104	ICI
Mo_2C	LTS	61	0.036	0.129	KIST
$Pt–Ni/CeO_2$	LTS	78	0.049	0.086	KIST

[a] Derived from N_2 adsorption study.
[b] Derived from CO chemisorption.

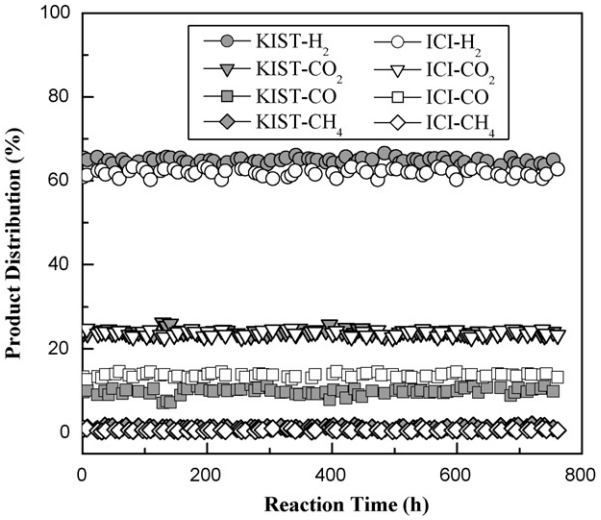

Fig. 3. Long-term stability of KIST and commercial catalysts in the ATR of *iso*-octane containing sulfur of less than 5 ppm [12]. Reaction temperature = 700 °C; space velocity = 8776 h^{-1}; feed molar ratios of $H_2O/C = 3$ and $O/C = 1$.

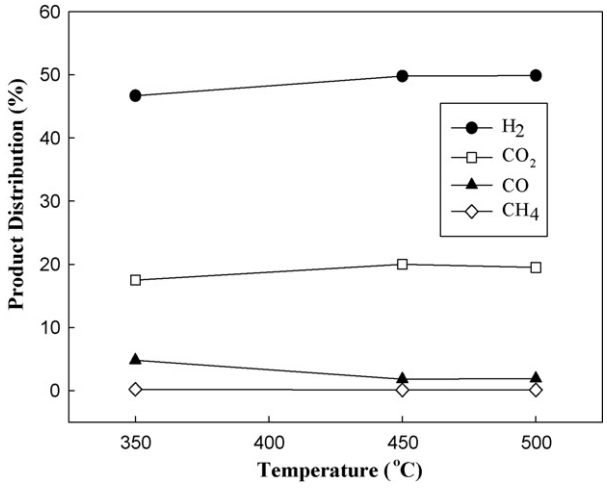

Fig. 4. The effect of reaction temperature on exit composition from WGS reaction over a HTS catalyst. Space velocity = 4227 h^{-1}, Feed composition: H_2 = 46.5%, CO = 8.4%, CO_2 = 14.8% balance with N_2 on a dry basis.

To elucidate the effect of sulfur impurities on the catalytic deactivation, ATR reaction of *iso*-octane containing sulfur of 100 ppm was investigated [12,13]. The KIST catalyst (Ni/Fe/MgO/Al_2O_3) was compared with the commercial ICI catalyst for sulfur tolerance in the ATR reaction of *iso*-octane (Cs = 100 ppm) at 700 °C, space velocity 8776 h^{-1} and feed molar ratios of $H_2O/C = 3$ and $O/C = 1$. $Ni/Fe/MgO/Al_2O_3$ catalyst displayed better sulfur tolerance than the commercial ICI catalyst, even though none of the systems was found to be completely sulfur resistant. There was no change in the product distributions for ATR of *iso*-octane over the KIST catalyst during the time period investigated. Thus, it was suggested that $Ni/Fe/MgO/Al_2O_3$ catalyst is an attractive ATR candidate for *iso*-octane fuel processor system.

3.2. HTS reaction

To increase the hydrogen concentration, the synthesis gas undergoes a water gas shift reaction where steam is reacted with CO to form H_2 and CO_2 as represented below:

$$CO + H_2O \rightarrow CO_2 + H_2$$

WGS reactors, charged with currently available commercial high temperature shift and low temperature shift catalysts, constitute about one third of the mass, volume and cost of the fuel processor system. The Partnership for a New Generation of Vehicles (PNGV) has set up a goal to reduce the weight of the shift reactors to 75%. Before the measurement of product distribution data from three different reaction stages, we carried out WGS reaction over a commercial HTS catalyst to find the individual reaction conditions for three different reaction stages. Fe_3O_4–Cr_2O_3 catalyst was used for the high temperature shift reaction. Fig. 4 shows the effect of reaction temperature on the product distribution for HTS reaction over the Fe_3O_4–Cr_2O_3 catalyst. The reactant compositions of WGS reactor were the exit compositions of ATR reactor: 46.5% H_2, 8.4% CO, 14.8% CO_2 balance with N_2 on a dry basis. The concentration of H_2 was found to be increased at the cost of the concentration of CO by means of WGS reaction. The product composition at 450 °C and space velocity of 4227 h^{-1} is 49.8% H_2, 1.8% CO and 20.0% CO_2. The exit gas from the HTS reactor in this system was cooled and passed into the LTS reactor as the reactant.

3.3. LTS reaction

Existing commercial LTS ($Cu–Zn/Al_2O_3$) catalyst, though highly active, is unsuitable for applications because of its large size and weight, and the deactivation tendency of an active metal under the severe conditions employed in fuel processor and hydrogen station systems. Molybdenum carbide and $Pt–Ni/CeO_2$ catalysts were used for the low temperature shift reaction, and were compared with a commercial LTS catalyst.

Molybdenum carbide catalyst was synthesized by the carburization of molybdenum oxide, and the carburization temperature of molybdenum oxide was determined by thermal gravimetric analysis (Sindo Science Co., TGA 2050) [16–18]. As the temperature reached 580 °C, MoO_3 converted to Mo_2C. The formation of carbide phase began at 580 °C and completed at 650 °C. Above 650 °C, excess of carbon was found to be deposited on the carbide system, thereby giving low activity. It was found that the activity of carbide catalysts in WGS reaction was greatly dependent on the carburization temperature. The optimum carburization temperature of molybdenum oxide for WGS reaction was found to be in the range of 640–650 °C.

It was observed that molybdenum carbide catalysts (ρ = 1.23–1.89 g/cm^3) have higher density than the commercial $Cu–Zn/Al_2O_3$ catalyst (ρ = 1.1 g/cm^3) [16]. Since molybdenum carbide catalyst showed higher gravimetric CO consumption rate than commercial LTS catalyst, Mo_2C catalyst is more promising candidate than commercial LTS catalyst as it leads to the reduction in volume of WGS reactor [16,17]. LTS reaction over $Pt–Ni/CeO_2$ catalyst was also carried out to develop an alternative to commercial LTS catalyst. It was found that $Pt–Ni/CeO_2$ catalyst (78 m^2/g) displayed high surface area over the commercial LTS catalyst (60 m^2/g).

We reported previously [16], KIST catalyst showed higher catalytic performance and thermal cycling stability than commercial LTS ($Cu–Zn/Al_2O_3$) catalyst. The LTS reaction of a feed containing 62.5% H_2, 31.8% deionized H_2O and 5.7% CO was carried out in temperature range of 200–300 °C with space velocity of 10,000 h^{-1}. The $Cu–Zn/Al_2O_3$ catalyst was reduced at 200 °C in a mixture of 2% H_2 in N_2 balance for 4.5 h and Mo_2C catalyst was reduced at 400 °C under the flow of H_2 for 4.5 h. The $Pt–Ni/CeO_2$ catalyst was reduced at 400 °C for 2 h under 5% H_2 in Ar balance at a flow rate of 40 cm^3/min. The activity of $Cu–Zn/Al_2O_3$ catalyst increased with increasing the reaction temperature up to 260 °C,

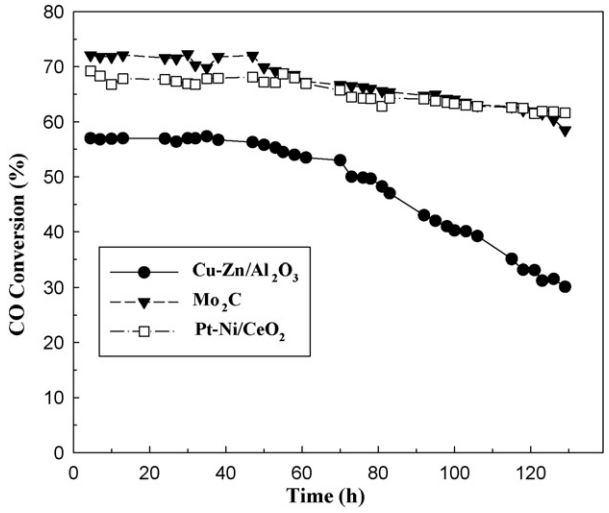

Fig. 5. The results of thermal cycling runs for LTS reaction over commercial Cu–Zn/Al_2O_3, KIST Mo_2C and Pt–Ni/CeO_2 catalysts [16]. The runs were performed at the reaction temperature of 250 °C over a time period of 130 h.

displayed the highest activity at 260 °C with CO conversion of 70%, and then decreased at high temperature over 260 °C [16]. Mo_2C and Pt–Ni/CeO_2 catalysts showed higher catalytic activity than commercial LTS catalyst at a temperature range of 200–300 °C and the activity progressively increased with increasing reaction temperature. Maximum activities of KIST catalysts were observed at 280–300 °C with a total CO conversion more than 85%.

Fig. 5 shows the thermal cycling run for LTS reaction over commercial Cu–Zn/Al_2O_3, Mo_2C and Pt–Ni/CeO_2 catalysts at 250 °C for 130 h [16]. To change the reduction and oxidation conditions of catalyst, the switch of electric furnace for heating WGS reactor was repeatedly operated on/off with some time intervals. CO conversion over Cu–Zn/Al_2O_3, Mo_2C and Pt–Ni/CeO_2 catalysts was found to be decreased progressively with a time on stream. All catalysts slowly deactivated during the thermal cycling run. In our previous work [12,14,16], we reported that Cu–Zn/Al_2O_3 catalyst was deactivated by sintering of active metal whereas Pt–Ni/CeO_2 catalyst was deactivated by the sintering of Ni particles during the thermal cycling test. The deactivation of Mo_2C catalyst during the

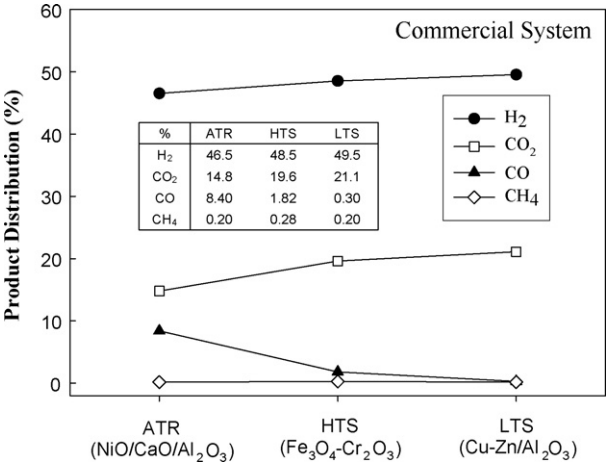

Fig. 6. The product distribution from three different reaction stages over the commercial catalyst system. The ATR reaction was carried out at temperature 700 °C, space velocity 8776 h^{-1}, molar ratios H_2O/C = 3 and O/C = 1. HTS and LTS reactions were carried out at 450 and 250 °C, respectively.

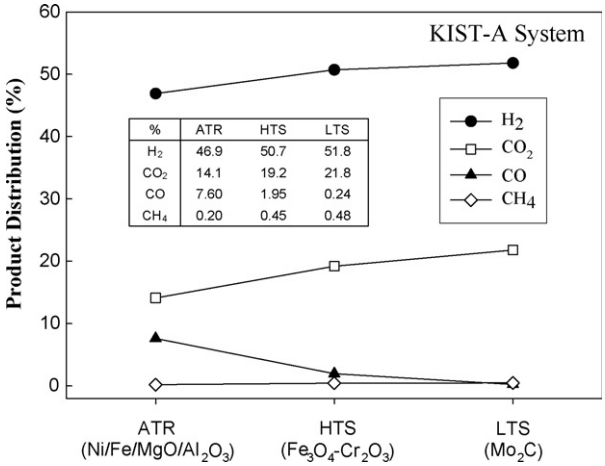

Fig. 7. The product distribution from three different reaction stages over the KIST-A catalyst system. The ATR over KIST catalyst was carried out at reaction temperature 700 °C, space velocity 8776 h^{-1}, molar ratios of H_2O/C = 3 and O/C = 1. HTS and LTS reactions were carried out at 450 and 250 °C, respectively.

thermal cycling run for LTS reaction was caused by transition of Mo_2C to molybdenum oxide or molybdenum oxy-carbide on the surface of Mo_2C with the reaction of H_2O in reactants. However, Mo_2C and Pt–Ni/CeO_2 catalysts showed higher stability than the commercial LTS catalyst (Cu–Zn/Al_2O_3). The CO conversion of Mo_2C and commercial LTS catalyst after the thermal cycling reaction for 130 h decreased by 8 and 17%, respectively. Characterization for structure of the catalysts before and after the thermal cycling reaction at 250 °C for 130 h was done using a XRD and TEM [12,16]. It was observed that Cu–Zn/Al_2O_3 catalyst was deactivated by sintering of active metal during the thermal cycling run. However, there was no major change in the XRD patterns and TEM images of Pt–Ni/CeO_2 and Mo_2C catalysts before and after the reaction [16]. Mo_2C and Pt–Ni/CeO_2 catalysts showed higher cycling stability than commercial Cu–Zn/Al_2O_3 catalyst.

3.4. *iso*-Octane fuel processor system

The WGS reaction is a critical step during the fuel processing since CO poisons the PEM electrode catalyst. To reduce the CO concentration, the reformate gas obtained from ATR of *iso*-octane undergoes a WGS reaction. The exit gas from the HTS reactor in this system was cooled and passed into the LTS reactor.

From the preliminary experimental results [9,14,16] and the recommendation from the catalyst manufacturer, the reaction temperatures used in HTS and LTS reactors were kept at 450 and 250 °C, respectively. The three different reactions over the commercial ICI, HTS and LTS catalysts were investigated. Fig. 6 shows the product distribution from three different reaction stages over the commercial catalysts system. The ATR reaction of *iso*-octane containing sulfur less than 5 ppm was carried out at 700 °C with a space velocity 8776 h^{-1} and molar ratios of H_2O/C = 3 and O/C = 1. Subsequently, HTS and LTS reactions were carried out at 450 and 250 °C, respectively. The concentrations of H_2 and CO_2 after the gases passed through HTS and LTS reactors increased, while those of CO and CH_4 decreased. The concentration of CO in hydrogen-rich stream was reduced to less than 3000 ppm as the reformate gas obtained from ATR of *iso*-octane over commercial ICI catalyst was passed through HTS and LTS reactors.

We observed that Ni/Fe/MgO/Al_2O_3 catalyst was found to be stable for the ATR of *iso*-octane during 760 h. Mo_2C and Pt–Ni/CeO_2 catalysts showed higher stability than the commercial LTS (Cu–Zn/Al_2O_3) during thermal cycling test [16]. Therefore, we have chosen

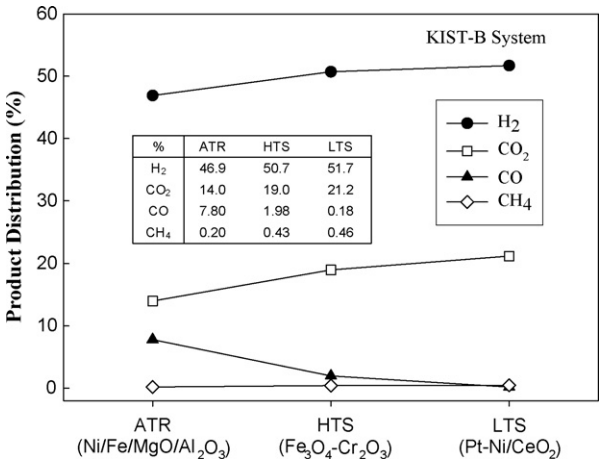

Fig. 8. The product distribution from three different reaction stages over the KIST-B catalyst system. The ATR over KIST catalyst was carried out at reaction temperature 700 °C, space velocity 8776 h^{-1}, molar ratios $H_2O/C = 3$ and $O/C = 1$. HTS and LTS reactions were carried out at 450 and 250 °C, respectively.

Table 2
Comparison of the KIST system with the commercial system for *iso*-octane fuel processor

Reformer system	Catalysts			CO content (ppm)
	ATR	HTS	LTS	
Commercial	$NiO/CaO/Al_2O_3$	Fe_3O_4–Cr_2O_3	$Cu–Zn/Al_2O_3$	3000
KIST-A	$Ni/Fe/MgO/Al_2O_3$	Fe_3O_4–Cr_2O_3	Mo_2C	2400
KIST-B	$Ni/Fe/MgO/Al_2O_3$	Fe_3O_4–Cr_2O_3	$Pt–Ni/CeO_2$	1800

KIST-A and KIST-B fuel processor system for *iso*-octane fuel processor for fuel cell-powered vehicles.

Figs. 7 and 8 show the product distributions from three different reaction stages over KIST-A and KIST-B reformer systems. KIST-A system was charged with ATR ($Ni/Fe/MgO/Al_2O_3$), commercial HTS (Fe_3O_4–Cr_2O_3) and LTS (Mo_2C) catalysts, and KIST-B system was charged with ATR ($Ni/Fe/MgO/Al_2O_3$), commercial HTS (Fe_3O_4–Cr_2O_3) and LTS ($Pt–Ni/CeO_2$) catalysts, respectively. It was found that the KIST fuel processor system with three different reaction stages was more active than those of the commercial catalysts. Especially, the concentration of CO in hydrogen-rich stream was reduced to less than 2400 ppm as the exit gas of *iso*-octane ATR over the KIST ($Ni/Fe/MgO/Al_2O_3$) catalyst was passed through commercial HTS and KIST LTS reactors. Table 2 shows the comparison of the KIST-A and KIST-B reformer systems with the commercial system for *iso*-octane fuel processor. The concentration of CO in the syngas for the commercial, KIST-A and KIST-B systems was found to be 3000, 2400 and 1800 ppm, respectively. The results suggest that the $Ni/Fe/MgO/Al_2O_3$ catalyst for ATR and $Pt–Ni/CeO_2$ catalyst for LTS were promising catalysts for development as the alternate commercial catalysts for the *iso*-octane fuel processor system. In order to reduce the concentration of CO in hydrogen-rich stream to less than 10 ppm especially for PEM fuel cell-powered vehicles applications, a preferential partial oxidation (PROX) reactor should be added to KIST fuel processor system.

4. Conclusions

We developed the *iso*-octane fuel processor system for fuel cell-powered vehicles applications, which charged with $Ni/Fe/MgO/Al_2O_3$ catalyst for ATR, Fe_3O_4–Cr_2O_3 catalyst for HTS and Mo_2C or $Pt–Ni/CeO_2$ catalyst for LTS reaction. It was found that the prepared catalyst formulations in the fuel processor system with three different reaction stages were more active than the commercial catalysts formulation. We could achieve the concentration of CO in the hydrogen-rich stream to less than 2400 ppm in the *iso*-octane fuel processor system charged with KIST ATR and LTS catalysts. The results suggest that the *iso*-octane fuel processor system of prepared catalysts can be applied to PEMFC system when a preferential partial integration oxidation reaction is added to KIST reformer system.

Acknowledgements

Funding for this work from KIST is greatly appreciated. We thank research group on gasoline reformer in KIST for helpful discussions.

References

[1] A. Docter, A. Lamn, J. Power Sources 84 (1999) 194.
[2] Arthur D. Little Inc., Multi-fuel Reformers for Fuel Cells Used in Transportation, Multi-fuel Reformers Phase I. Final Report, DOE/CE/50343-2, 1994.
[3] A.E. Borroni-Bird, Soc. Auto Eng. 762 (1995) 2118.
[4] Y.K. Sun, W.Y. Lee, Korean J. Chem. Eng. 12 (1995) 36.
[5] D. Peter, M. Alexander, J. Power Sources 167 (2007) 472.
[6] A.-M. Azad, M.J. Duran, A.K. McCoy, M.A. Abraham, Appl. Catal. A 332 (2007) 225.
[7] S. Kazuhiro, F. Kaoru, Catal. Comm. 8 (2007) 1697.
[8] T.J. Flynn, R.M. Privette, M.A. Perna, K.E. Kneidel, D.L. King, M. Cooper, Soc. Autom. Eng. 1999-01-0536 (1999) 47.
[9] D.J. Moon, J.W. Ryu, S.D. Lee, B.S. Ahn, S.I. Hong, in: Proceedings of the 2002 Fuel Cell Seminar, 2002, p. 348.
[10] L. Lloyd, D.E. Ridler, M.V. Twigg, Catalyst Handbook, 2nd ed., Wolfe Publ. Ltd., England, 1989, p. 308.
[11] W. Ructtinger, O. Ilinich, R.J. Farrauto, J. Power Sources 52 (2003) 1.
[12] D.J. Moon, J.W. Ryu, Catal. Lett. 89 (2003) 207.
[13] D.J. Moon, J.W. Ryu, S.D. Lee, B.S. Ahn, Korea Patent 2001-8494 (2002).
[14] D.J. Moon, K. Sreekumar, S.D. Lee, B.G. Lee, H.S. Kim, Appl. Catal. A 215 (2001) 1.
[15] D.J. Moon, J.W. Ryu, S.D. Lee, B.G. Lee, B.S. Ahn, in: Proceedings of the 9th APPChE Congress & CHEMECA, 2002.
[16] D.J. Moon, J.W. Ryu, Catal. Lett. 92 (2004) 17.
[17] J. Patt, D.J. Moon, C. Phillips, L. Thompson, Catal. Lett. 65 (2000) 193.
[18] L. Thompson, J. Patt, D.J. Moon, C. Phillips, U.S. Patent 0013221 A1 (2002).